

Lawrence Berkeley National Laboratory

Lawrence Berkeley National Laboratory

Title

Genomic deletion of a long-range bone enhancer misregulates sclerostin in Van Buchem disease

Permalink

<https://escholarship.org/uc/item/022699dt>

Authors

Loots, Gabriela G.
Kneissel, Michaela
Keller, Hansjoerg
[et al.](#)

Publication Date

2005-04-15

Peer reviewed

Genomic deletion of a long-range bone enhancer misregulates *sclerostin* in
Van Buchem disease

Gabriela G. Loots^{1*‡}, Michaela Kneissel², Hansjoerg Keller², Myrna Baptist², Jessie
Chang^{1‡}, Nicole M. Collette[‡], Dmitriy Ovcharenko¹, Ingrid Plajzer-Frick¹ and Edward M.
Rubin^{1,3}

¹Life Sciences Division

Lawrence Berkeley National Laboratory

One Cyclotron Road

Berkeley, CA 94720

²Novartis Institutes for BioMedical Research, Bone Metabolism, Basel, Switzerland.

³DOE, Joint Genome Institute, Walnut Creek, CA, USA.

[‡]Current Address:

Genome Biology Division,

Lawrence Livermore National Laboratory

7000 East Avenue, L-441

Livermore, CA 94550

*Correspondence should be addressed to G.G. Loots: loots1@llnl.gov

Running title:

Sclerostin regulation in Van Buchem disease

ABSTRACT

Mutations in distant regulatory elements can negatively impact human development and health, yet due to the difficulty of detecting these critical sequences we predominantly focus on coding sequences for diagnostic purposes. We have undertaken a comparative sequence-based approach to characterize a large noncoding region deleted in patients affected by Van Buchem disease (VB), a severe sclerosing bone dysplasia. Using BAC recombination and transgenesis we characterized the expression of human *sclerostin* (*sost*) from normal (hSOST^{wt}) or Van Buchem (hSOST^{vbΔ}) alleles. Only the hSOST^{wt} allele faithfully expressed high levels of human *sost* in the adult bone and impacted bone metabolism, consistent with the model that the VB noncoding deletion removes a *sost*-specific regulatory element. By exploiting cross-species sequence comparisons with *in vitro* and *in vivo* enhancer assays we were able to identify a candidate enhancer element that drives human *sost* expression in osteoblast-like cell lines *in vitro* and in the skeletal anlage of the E14.5 mouse embryo, and discovered a novel function for *sclerostin* during limb development. Our approach represents a framework for characterizing distant regulatory elements associated with abnormal human phenotypes.

Deleterious mutations in distant regulatory elements postulated to dramatically impact human development and health have been minimally explored. This problem is in large part due to the fact that there are no simple ways to discern regulatory elements from nonfunctional sequences or to ascertain whether mutant phenotypes are caused by regulatory mutations. Among Mendelian disorders associated with noncoding mutations only a few cases are described that clearly link alterations in distant *cis*-acting regulatory regions to the cause of the disease (Enattah et al. 2002; Ionasescu et al. 1996; Lettice et al. 2003; Tsui et al. 2003; Wang et al. 2000), and these documented cases predominantly correspond to large chromosomal aberrations (Chuzhanova et al. 2003; Cimborra et al. 2000; Curtin et al. 1985; Curtin and Kan 1988; Kleinjan et al. 2001). Structural variation in the human genome described as large-scale polymorphisms has been recently shown to be more common than previously anticipated (Sebat et al. 2004), therefore the extent to which large noncoding duplications and deletions impact human biology remains a largely unanswered question. In this study, we demonstrate that a very important skeletal dysplasia, Van Buchem (VB) disease, associated with a large noncoding deletion is caused by the removal of a bone-specific distant enhancer element.

Van Buchem disease (MIM 239100) is a homozygous recessive disorder (Balemans et al. 2002; Staehling-Hampton et al. 2002; Van Hul et al. 1998) that maps to chromosome 17p21 and results in progressive increase in bone density (Wergedal et al. 2003). The accumulation of bone mass gives rise to facial distortions, enlargement of the mandible and head, entrapment of the cranial nerves, increase in bone strength, and excessive weight (Balemans et al. 2002; Staehling-Hampton et al. 2002; Van Hul et al. 1998). Sclerosteosis (MIM 269500) is a cranio-tubular hyperostosis that is

phenotypically indistinguishable from Van Buchem disease (VB) except that it is more severe and occasionally displays syndactyly of the digits (Balemans et al. 1999; Beighton et al. 1977; Brunkow et al. 2001; Hamersma et al. 2003; Kusu et al. 2003), a trait absent in VB patients.

An exciting development has been the recent discovery of a novel protein that acts as a negative regulator of bone formation, *sclerostin* (*SOST*) (Balemans et al. 2001; Brunkow et al. 2001), whose expression is affected in both sclerosteosis and Van Buchem disease. Whereas sclerosteosis patients carry homozygous null *sost* mutations, VB patients lack any *sost* coding mutations (Staehling-Hampton et al. 2002; Van Bezooijen et al. 2004; Winkler et al. 2003). They do however, carry a homozygous 52 kb noncoding deletion (*vbΔ*) ~35kb downstream of the *sost* transcript and ~10kb upstream of the downstream gene, *meox1*, on human chromosome 17p21 (Figure 1A) (Balemans et al. 2002; Staehling-Hampton et al. 2002). The shared clinical similarities between VB and sclerosteosis along with their strong genetic linkage to the *sost* locus on chromosome 17q12 suggests that they are allelic, and that the deletion in VB patients removes an enhancer element essential for directing the expression of human *sost* in the adult skeleton. To gain insight into the mechanism by which this newly discovered gene impacts bone patterning and remodeling in Van Buchem disease, as well as to characterize the transcriptional regulation of *sclerostin* we have characterized human BAC *sost* transgenic mice carrying either a normal (hSOST^{wt}) or an allele with the VB associated deletion (hSOST^{vbΔ}). Only the hSOST^{wt} allele faithfully expresses human *sost* in the adult bone and impacts bone metabolism, consistent with the model that the VB noncoding deletion removes a *sost*-specific regulatory element. By exploiting cross-

species sequence comparisons with *in vitro* and *in vivo* enhancer assays we have identified a potential enhancer element that drives human *sost* expression in the skeletal anlage, and discovered a novel function for *sclerostin* during limb development, demonstrating that this very important skeletal dysplasia, Van Buchem disease, is caused by the removal of bone-specific distant enhancer elements and is allelic to sclerosteosis.

Results

Molecular and Phenotypic Characterization of Van Buchem transgenic mouse models

A ~158 kb human BAC (RP11-209M4) (hSOST^{wt}) encompassing the 3' end of the *DUSP3* gene, *sost*, *meox1*, and the ~90kb noncoding intergenic interval separating *sost* from the neighboring gene, *meox1*, was engineered using homologous recombination in bacteria (Lee et al. 2001) to delete the 52kb region missing in VB patients and to create a construct that mimics the VB (hSOST^{vbΔ}) allele (Figure 1A). Three independent founder lines of each transgenic construct were generated using standard transgenic procedures (Nobrega et al. 2003). Similar to the endogenous mouse *sost* expression, and the reported human expression (Balemans et al. 2001; Brunkow et al. 2001) all lines of hSOST^{wt} transgenic animals reliably expressed human *sost* in the mineralized bone of neonatal and adult mice (skull, rib and femur), while all of the hSOST^{vbΔ} lines had dramatically reduced levels of human *sost* mRNA expression; as determined by rtPCR and qPCR. All lines (hSOST^{wt} and hSOST^{vbΔ}) also consistently expressed human *sost* in the adult kidney and heart. Here, we present data on the top expressing lines from each transgenic construct, which are referred to in the manuscript as A and B version of each transgene (Figure 1B). Expression in the lung, brain and spleen varied among lines, while no BAC transgenic line expressed in the liver contrary to the reported human tissue-specific expression (Brunkow et al. 2001). These data demonstrate that *in vivo*, the VB allele confers dramatically reduced *sost* expression in the adult bone and suggests that the vbΔ contains essential bone-specific enhancer elements.

Sclerostin is an osteocyte-expressed negative regulator of bone formation that is structurally most closely related to the DAN/Cerberus family of BMP antagonists (Van

Bezooijen et al. 2004; Winkler et al. 2003). Several members of this family including *noggin* and *gremlin* are expressed embryonically in the developing limb (Brunet et al. 1998; Khokha et al. 2003), therefore we examined human *sost* expression in the early mouse embryo. rtPCR analysis of RNA isolated from whole embryos showed high levels of human *sost* expression in all lines from both hSOST^{wt} and hSOST^{vbΔ} transgenic animals (Figure 1C). *Sost* expression precedes endochondral ossification, and was detected as early as E9.5. Since the VB deletion did not impact human *sost* embryonic expression, we used E10.5 embryonic RNA to quantify the level of transgene expression in different hSOST^{wt} and hSOST^{vbΔ} transgenic founder lines (Figure 1D). Comparable expression levels were also confirmed in the kidneys of hSOST^{wt} and hSOST^{vbΔ} animals. This data strengthens the evidence that the lack of human *sost* bone expression in hSOST^{vbΔ} animals is dependent on the 52kb noncoding deletion, rather than reflecting an artifact due to transgene copy number or site of integration.

The availability of BAC transgenic animals carrying wildtype and VB alleles also allowed us to address whether the other gene flanking the vbΔ region, the transcription factor *meox1* is affected by removing the 52kb vbΔ. *Meox1* has been previously shown to be involved in skeletal myogenesis (Mankoo et al. 2003; Petropoulos et al. 2004), therefore it has been uncertain whether it also plays a role in the phenotypic outcomes of Van Buchem Disease, particularly since previous experiments using human patient samples prevented researchers from directly examining the effect of the noncoding deletion on gene expression (Staehling-Hampton et al. 2002). We have examined *meox1* expression in all available transgenic lines from both hSOST^{wt} and hSOST^{vbΔ} constructs, and unfortunately were not able to detect any significant human *meox1* expression in

adult tissues (data not shown). Based on these results, we have concluded that the 209M4 BAC does not possess sufficient *meox1*-specific regulatory elements to recapitulate the wildtype human *meox1* expression in the hSOST^{wt} transgenics, therefore, our experiments can not evaluate the impact the VB deletion has on *meox1* expression.

Since lack of sclerostin causes increased bone density (Brunkow et al. 2001), we investigated whether elevated levels of human sclerostin have opposite effects on bone mass. Consistent phenotypic data has been obtained for both lines A and B of hSOST^{wt} and hSOST^{vbΔ} transgenic constructs (Figure 2; Supplementary Materials). Animals from these lines expressed equivalent amounts of embryonic human *sost* (Figure 1D; gray shaded bars). For the rest of the manuscript we will refer for these mice as hSOST^{wt} and hSOST^{vbΔ}. hSOST^{wt} transgenics grew to skeletal maturity with normal body size and weight (Figure 2A) however, the animals displayed decreased bone mineral density (BMD) in the appendicular and axial skeleton, as evaluated by dual energy X-ray absorptiometry (DEXA) analysis (Figure 2B). Micro-Computed-Tomography (microCT) analysis of three-dimensional cancellous bone structures revealed that the mice have decreased bone volume, trabecular number, thickness and increased trabecular separation (Figure 2C). In contrast, the bone parameters of hSOST^{vbΔ} transgenics were indistinguishable from non-transgenic littermate controls. The observed osteopenia was gene dose dependent. hSOST^{wt} transgenic mice bred to homozygosity revealed a further dramatic decrease in tibial cancellous bone volume (Figure 3A, C). Histomorphometric analysis revealed that these animals display further decreased bone formation rates at skeletal maturity reflected in decreased fluorochrome marker uptake into mineralizing bone both in cancellous (Figure 3B, D) and cortical bone (tibia: non-tg = 0.319 +/- 0.016

$\mu\text{m}/\text{day}$ versus $\text{hSOST}^{\text{wt/wt}} = 0.110 \pm 0.027 \mu\text{m}/\text{day}$ $p < .001$) in both the appendicular (Figure 3B,C) and the axial skeleton. Either the number of terminally differentiated bone forming cells, the osteocytes, or the number of bone resorbing cells, the osteoclasts, were significantly affected by the transgene expression (data not shown).

In contrast to hSOST^{wt} transgenics, $\text{hSOST}^{\text{vb}\Delta}$ animals did not display an osteopenic bone phenotype in neither the appendicular nor the axial mature skeleton, even in the homozygous configuration (Figure 2B,C; Supplementary Materials). These data demonstrate that modulation of *sost* expression dramatically impacts bone formation in the adult mammalian skeleton. Most importantly, these phenotypic data suggest that overexpressing human *sost* under the control of its own proximal promoter elements in concert with the downstream VB region negatively modulates adult bone mass. In contrast, bone mass is unaffected in transgenic animals that lack the 52kb VB region, in a construct that mimics the allele carried by VB patients, consistent with the model that Van Buchem disease is caused by removing a bone-specific regulatory element.

Interestingly, and consistent with the observed embryonic expression, elevated levels of human *sost* result in abnormal digit development in both hSOST^{wt} and $\text{hSOST}^{\text{vb}\Delta}$ BAC transgenics bred to homozygosity. The fore- and hind-limbs of these animals display a wide range of fused and missing digits as visualized by autoradiography (data not shown) and μCT (Figure 4B). rtPCR data correlates *SOST* expression with the severity of digit abnormalities (data not shown). Mouse whole mount *in situ* hybridization revealed *sost* to be expressed as early as embryonic stage 9.5 (E9.5), predominantly in the mesenchymal tissue of the developing limb bud (Figure 4A). These findings imply that *sost* embryonic expression is controlled by a transcriptional

regulatory element different from the one driving the adult bone expression, consistent with the observation that both sclerosteosis and VB patients suffer from abnormal bone mass accumulation while only sclerosteosis patients exhibit syndactyly of the digits (Staehling-Hampton et al. 2002).

Comparative Sequence Analysis and Enhancer Assays

Given the striking bone phenotypes observed in both VB and sclerosteosis patients, we next focused on the identification of noncoding sequences required for *sost* bone-specific expression through a combination of comparative sequence analysis and transient transfection assays. We aligned a ~140kb human *SOST* region (<http://zpicture.dcode.org/>) (Ovcharenko et al. 2004) (RP11-209M4; AQ420215, AQ420216) to the corresponding mouse sequences from chromosome 11 (Mouse chr11:101,489,231-101,688,385; Oct.03 Freeze) (Figure 5A). A stringent requirement of at least 80% identity over a 200 base pair (bp) window ($\geq 80\%ID$; $\geq 200bp$) identified seven evolutionarily conserved regions (ECR2-8) within the *vbΔ* genomic interval, which were prioritized for *in vitro* enhancer analysis. ECR2-8 were tested for their ability to stimulate a heterologous promoter (SV40) in osteoblastic (UMR-106) and kidney (293) derived cell lines. One element, ECR5, was able to stimulate transcription in UMR106 cells (Figure 5B), but not in the kidney cell line, suggesting that ECR5 enhancer function is specific to the osteoblastic lineage. We also tested the transcriptional activity of the human *sost* proximal promoter region (2kb region upstream of 5'UTR) in the two cell types and compared it to the SV40 and the osteoblast-specific *osteocalcin* promoter (*OG2*). The SV40 promoter showed comparable activity in both cell lines and, as

expected, *OG2* was only active in the UMR-106 cells. The human *sost* promoter stimulated transcription in the osteoblastic cells similarly albeit slightly higher activity than the *OG2* promoter, while it demonstrated a threefold stronger activity in kidney cells (Figure 5B). These data suggest that *sost* kidney expression may be due to proximal promoter sequences, whereas strong expression in osteoblast cells requires the activity of the ECR5 element. Consistent with the results obtained from transfecting SV40 promoter constructs, only ECR5 was capable of activating the human *sost* promoter (4X) in UMR106 cells (Figure 5C), while all other ECR-constructs had background level expression. Thus, a small sequence element within the *vbΔ* region (ECR5) was identified that confers *in vitro* osteoblast-specific enhancer activity onto both the human *sost* and the SV40 heterologous promoter.

To test ECR5's ability to drive expression in the skeletal structures of the mouse embryo we expressed a ECR-*hsp68-LacZ* construct in transgenic mice (Figure 5D) (Nobrega et al. 2003). Transient transgenic animals were created using standard techniques (Mortlock et al. 2003) and F0 pups were stained for *β-galactosidase* expression at E14.5 (Nobrega et al. 2003). Transgenic embryos expressed *LacZ* in the cartilage of the ribs, vertebrae and skull plates (Figure 5D) and the expression was identical in all positive transgenic embryos obtained from two independent injections (N=2). In parallel we also injected ECR4- and ECR6-*hsp68-LacZ* constructs and assayed *LacZ* expression at E12.5 and E14.5. None of the ECR4 (N=6) and ECR6 (N=2) positive embryos expressed *LacZ* at these time points. These data highly suggest that the 250 basepair (bp) ECR5 element contained within the 52 kb deleted in Van Buchem patients functions to drive *sost* bone-specific expression *in vivo*.

Discussion

Sclerosing bone dysplasias are rare genetic disorders in which excessive bone formation occurs due to defects in bone remodeling (Van Hul et al. 2001). Identifying the responsible genes, their regulation and mechanisms of action will provide useful insights into bone physiology and potentially benefit the treatment of these disorders, as well as facilitate the development of therapies for replenishing bone loss in osteoporosis. In this study we have demonstrated that the 52 kb noncoding deletion present in Van Buchem patients removes a distant *sost*-specific regulatory element and therefore Van Buchem disease is hypomorphic to sclerosteosis. Currently, we don't have a clear view of how the lack of sclerostin promotes osteogenesis, therefore elucidating its transcriptional regulation is key to understanding the interconnection between its expression pattern in osteogenic cells and its mode of action either as a BMP-antagonist (Winkler et al. 2003) or WNT-antagonist. The elaborate expression pattern we detect along with the multitude of putative enhancer elements that have the potential to positively or negatively impact *sost* in a spatial and temporal precise manner attest to this molecule's complexity and functional versatility. Consistent with this view, our analysis provides robust *in vivo* evidence for the role of sclerostin during bone formation, modulation of adult bone mass and for a novel function during limb development.

In general, the osteopenic phenotype we observed is consistent with reports describing transgenic mice overexpressing BMP-antagonists from cDNA constructs driven by *osteocalcin* (*OG2*) promoter (Devlin et al. 2003; Winkler et al. 2003). Unlike *OG2*>hSOST transgenic animals (Winkler et al. 2003), we never observed architectural disorganization of the lumbar vertebrae. We believe the osteopenic phenotypic variations

between the cDNA and BAC *sost* transgenic mice are most likely attributed to the transcriptional control of human *sost* in each transgenic construct. hSOST^{wt} BAC transgenics more faithfully mirror the proper regulatory control exerted on the *sost* gene in the endogenous context of the human genome, while the *OG2*>hSOST transgenic expression is ectopic and highlights the transcriptional specificity of the *osteocalcin* promoter.

Since sclerosteosis is caused by *sost* null mutations (Balemans et al. 2001; Brunkow et al. 2001), our results indicate that VB disease and sclerosteosis are allelic, VB patients are hypomorphic for the *sost* gene and lack *sost* expression in the adult bone. Our data suggests that *sost* embryonic expression is unaltered in VB patients, who also never display syndactyly of the digits, indicating that both reduced and elevated levels of human sclerostin negatively impact limb development and digit formation, a novel function attributed to this molecule.

Our findings provide evidence that noncoding regions in the VB deletion control Sclerostin expression levels and modulate BMD in mice, therefore an important question is whether variation in BMD in the general population could also be directly impacted by sequence variants in key noncoding regions of the VB deletion. A recent new study investigated the association between common polymorphisms in the *sost* gene region with BMD in elderly whites (Uitterlinden et al. 2004). From a set of 8 polymorphisms, one 3-bp deletion (SRP3) from the *sost* promoter region was associated with decreased BMD in women, and a polymorphic variant (SRP9) from the VB deletion region was associated with increased BMD in men. Whereas this SRP9 does not map on any human-mouse conserved region in the VB deletion, an important question for future studies is

whether this SNP is in linkage disequilibrium with ECR5 or if additional functional SNPs could be identified in this or other *sost*-specific enhancer elements.

The genetic factors that contribute to susceptibility to bone loss are extremely heterogeneous, therefore murine models that affect bone development and growth can provide invaluable insights into the molecular mechanisms of progressive bone loss in humans. Human genetic diseases of the skeleton such as sclerosteosis and Van Buchem disease provide a starting point for understanding the modulation of anabolic bone formation, and ultimately have the potential to identify key molecular components that can be used as new therapeutic agents to treat individuals suffering from bone loss disorders. Our study also provides strong support for the utilization of comparative sequence analysis to dramatically filter through nonfunctional regions in the human genome and enhance the discovery of noncoding disease-causing mutations both in discrete enhancer elements or in large noncoding deletions. This study represents a clear and unambiguous case where altering noncoding genomic content deleteriously impacts gene expression, demonstrating that mutations in distant regulatory elements are able to cause congenital abnormalities analogous to coding mutations.

Methods

Generating Transgenic Mice

FRT-kan-FRT cassette was excised from pICGN21 vector (KpnI; SacI) and inserted into pUC18 to create pUC18.kan.FRT. Homologous arms were PCR-amplified from 209M4 BAC DNA and cloned into pUC18.kan.FRT vector using EcoRI/SacI sites for the left arm (VBDelH1: fwd 5'-TTGGTACCGGATTGAAGTGATCCCCAGCTGGA-3'; rvd 5'-TTGAGCTCCAATCTCCTGACCTTGTGATCCGC-3'), and the SmaI site for the right arm (VbDelH2: fwd 5'-TTCCCGGGCGCTTGAACCCAGTAGGTGGAGG-3'; rvd 5'-TTCCCGGGTACCAAGGGATGGACAGAAGACAGGCAG-3') to create the recombination vector pUC18.kan.FRT.VBDel. 200-300 ng KpnI digested VBDelH1-FRT-kan-FRT-VbDelH2 fragment was electroporated into EL250-209M4 cells.

Recombinant BACs were identified by PCR and pulse-field gel analysis, were isolated at a final concentration of 1 ng/ml and microinjected into fertilized FVB mouse eggs using standard procedures. Transgenic mice were genotyped using PCR analysis of DNA prepared from tail DNA of founder animals using the following primer pair: 5'-ATGTCCACCTTGCTGGACTC-3' and 5'-GTCTGTGGGCTGGTTTGCAT-3'. Transgenic mice were maintained on FVB background.

RT-PCR, Quantitative RT-PCR and in situ hybridization

Total RNA was isolated with Trizol reagent (Invitrogen) and reverse-transcribed into cDNA (Superscript II, Gibco) using standard methods. cDNA was amplified using GC-Melt PCR kit (Clontech; 65°C annealing/3 min extension/35 cycles] using human (fwd 5'-AGAGCCTGTGCTACTGGAAGGTGG-3', rvd 5'-TAGGCGTTCTCCAGCTCGGCC-

3') and mouse (fwd 5'-GACTGGAGCCTGTGCTACCGA-3', rvd 5'-CTTGAGCTCCGACTGGTTGTGGAA-3') SOST primer sets. Mouse beta-actin (fwd 5'-CCTCTATGCCAACACAGTGC-3', rvd 5'-CTGGAAGGTGGACAGTGAGG-3') was used as control [58°C annealing/30 sec extension/25 cycles]. Quantitative rtPCR expression analysis was performed using an ABI Prism 7900HT sequence detection system, TaqMan® Universal PCR Master mix, human 18S rRNA pre-developed TaqMan® assay reagent for normalization and TaqMan® Assay-on-Demand™ products for mouse, rat and human SOST all from Applied Biosystems. We considered noon on the day that we found a vaginal plug to be E0.5. We carried out RNA localization by whole-mount *in situ* hybridization according to established protocols. RNA antisense probes were labeled with digoxigenin and were synthesized with T7 RNA polymerase as previously described.

Dual energy X-ray absorptiometry (DEXA) analysis.

Tibial, femoral and lumbar vertebral bone mineral density (in milligrams per square centimeter) was measured using a regular Hologic QDR-1000 instrument (Hologic, Waltham, Mass., USA). A collimator with 0.9-cm-diameter aperture and an ultrahigh resolution mode (line spacing, 0.0254 cm; resolution, 0.0127 cm) were used. The excised long bones were placed in 70% alcohol onto a resin platform provided by the company for soft tissue calibration. Daily scanning of a phantom image controlled the stability of the measurements. Instrument precision and reproducibility had been previously evaluated by calculating the coefficient of variation of repeated DEXA and had been found to be below 2%. Coefficients of variation were 0.5 to 2% for all evaluated

parameters. A set of 5-month-old male mice was analyzed (non-tg = 13 littermates of all analyzed lines, hSOST^{wt} = 15 (heterozygous mice from 2 hSOST^{wt} BAC lines, hSOST^{vbΔ} = 14 off-springs of heterozygous matings from 2 hSOST^{vbΔ} lines).

Micro computed tomography (microCT) analysis.

Cancellous bone structure was evaluated in the proximal tibia metaphysis using a Scanco vivaCT20 (Scanco Medical AG, Bassersdorf, Switzerland). The nonisometric voxels had a dimension of 12.5μm x 12.5μm x 12.5μm. From the cross-sectional images the cancellous bone compartment was delineated from cortical bone by tracing its contour at every 10th section. In all the other slices boundaries were interpolated based on the tracing to define the volume of interest. 660 slices covering a total length of 0.8mm within the area of the secondary spongiosa (1.3mm from the proximal end) were evaluated. A threshold value of 175 was used for the three dimensional evaluation of trabecular number, thickness, and separation. Both sets of male 5-month-old mice on which DEXA and histomorphometric analysis has been performed were analyzed. A voxel size of 25μm x 25μm x 25μm was chosen for visualization of the digits of the fore- and hind limbs.

Histomorphometric analysis.

After dissection, the tibia and lumbar vertebrae were placed for 24h in Karnovsky's fix, dehydrated in ethanol at 4°C, and embedded in methylmethacrylate. A set of 4- and 8-, microm-thick nonconsecutive microtome sections were cut in the frontal midbody plane for evaluation of fluorochrome-label-based dynamic and cellular parameters of bone

turnover. The 4 microm-thick sections were stained with TRAP and Giemsa stain. The sections were examined using a Leica DM microscope (Leica, Glattbrugg, Switzerland) fitted with a camera (SONY DXC-950P, Tokyo, Japan) and adapted Quantimet 600 software (Leica, Cambridge, UK). Two sections/animal were sampled for all sets of parameters. Microscopic images of specimens were evaluated semiautomatically digitally (X400 magnification). All parameters were measured and calculated according to Paritt et al. 1987 (J Bone Min Res). Fluorochrome label bone formation dynamics were evaluated on unstained 8 microm-thick sections. Bone perimeter, single- and double-labeled bone perimeter, and interlabel width were measured. Mineralized perimeter (%), mineral apposition rates (micrometers/day) (corrected for section obliquity in the cancellous bone compartment), and daily bone formation rates (daily bone formation rate/bone perimeter [micrometer/day]) were calculated. Osteoclast numbers (osteoclast number/bone perimeter [millimeters⁻¹]) and perimeter values (osteoclast perimeter/bone perimeter [percent]) were determined on the TRAPstained slides, and osteocyte number (osteocyte number/bone perimeter [millimeters⁻¹]) on the Giemsa stained slides. All parameters were evaluated in the spongiosa and at the endocortex. A set of 5-month-old male mice from one hSOSTw line was analyzed (non-tg = 5, hSOSTwt/+ = 7, hSOSTwt/wt = 4).

In vitro Enhancer Assays

ECRs were PCR-amplified with 5'NheI-linkers, TOPO-cloned into pCR2.1 vector (Invitrogen) then shuttled into NheI/XhoI sites of pGL3-promoter (Promega) or HindIII/PstI of hsp68-LacZ (B. Black). The following primers were used to amplify

human DNA (62°C annealing/30 sec extension/35 cycles): ECR2 (545 bp) 5'-AGCAACGCAGGGCAGGAGCCAAGA-3', 5'-TAGCTGGCCTCTCCTGGGCGTCTT-3'; ECR3 (410 bp) 5'-GGGGGCTGTATGGAAAGGAGACAT-3', 5'-CTTGAGCAGTAGGGCCAAGCCCT-3'; ECR4 (296 bp) 5'-TGACAAACAGGAAGGTGGCAGGGC-3', 5'-CCCCAACATTCTGTCCCCTTG-3'; ECR5 (259 bp) 5'-TCCTTGCCACGGGCCACCAGCTTT-3', 5'-CCCCCTCATGGCTGGTCTCATTTG-3'; ECR6 (666 bp) 5'-CCCTGAGAAACATGCCTCTGTCCC-3', 5'-CTTAGCAATCTGGGTGACCCTGGG-3'; ECR7 (568 bp) 5'-AAACTGCCAAGCCCCAGCTGGCTA-3', 5'-GCCCAGGGCTCAGAAATGTGTGGA-3'; ECR8 (352 bp) 5'-TTCCTACCAAGGTGGCTGCCACC-3', 5'-CCTTCAGAGAAGCAAATGGCTGGGG-3'; -2kb promoter 5'-CAGCAGAAGATGTCACAGCAGG-3', 5'-GAGCTGCATGGTACCAGCCAGA-3'. Human SOST promoter sequence (2kb upstream of 5'UTR) was PCR-amplified with SmaI-linkers and transferred into the SmaI site of pGL3basic (Promega). A luciferase reporter plasmid containing mouse *osteocalcin* (*OG2*) promoter sequence from -1323 to +10 in pGL3basic was kindly obtained from B. Fournier (Novartis Basel, Switzerland). Reporter plasmids containing ECR-4, -5 or -6 upstream of the human *sost* promoter were generated by inserting the ECR elements into the NheI site. Plasmid DNA was isolated using standard endotoxin-free methods (Qiagen). FuGene (Roche) and a CMV-bgal reporter plasmid (Clontech) as internal control were used for transient transfections of rat UMR-106 and human 293 cells. Cells were incubated for 24 hours at 37°C and luciferase and galactosidase expression were measured using standard assay kits (Promega).

Transient transgenic analysis

500 ng of DNA was linearized with NotI, followed by CsCl gradient purification and 2-5 ng was used for pronuclear injections of FVB embryos. E12.5-E14.5 embryos were dissected in ice-cold PBS, and were fixed in 4% paraformaldehyde at 4°C for 1-2 hours and stained for *LacZ* as described. Transgenic embryos were detected by PCR from tail DNA [fwd 5'-TTTCCATGTTGCCACTCGC-3', revd 5'-AACGGCTTGCCGTTTCAGCA-3'; 55°C annealing/30 sec extension/25 cycles].

Acknowledgements

The authors would like to thank M. Bruederlin, E. Kuhn, M. Merdes, A. Studer, and J. Wirsching for excellent technical help and B. Fournier for sharing the mouse osteocalcin reporter plasmid. Many thanks to M. Brunkow and D. Winkler for providing us with the original 209M4 human BAC. The authors are deeply indebted to Lisa Stubbs, Richard Harland, Mustafa Khokha and Marcelo Nobrega for invaluable advice and comments on the manuscript. G.G.Loots was supported by the Department of Energy Alexander Hollaender Fellowship and by NIH (HD47853-01). This work was performed under the auspices of the U.S. Department of Energy by the University of California, Lawrence Berkeley National Laboratory Contract No. AC0376SF00098.

REFERENCES

- Balemans, W., M. Ebeling, N. Patel, E. Van Hul, P. Olson, M. Dioszegi, C. Lacza, W. Wuyts, J. Van Den Ende, P. Willems, A.F. Paes-Alves, S. Hill, M. Bueno, F.J. Ramos, P. Tacconi, F.G. Dikkers, C. Stratakis, K. Lindpaintner, B. Vickery, D. Foernzler, and W. Van Hul. 2001. Increased bone density in sclerosteosis is due to the deficiency of a novel secreted protein (SOST). *Hum Mol Genet* **10**: 537-543.
- Balemans, W., N. Patel, M. Ebeling, E. Van Hul, W. Wuyts, C. Lacza, M. Dioszegi, F.G. Dikkers, P. Hildering, P.J. Willems, J.B. Verheij, K. Lindpaintner, B. Vickery, D. Foernzler, and W. Van Hul. 2002. Identification of a 52 kb deletion downstream of the SOST gene in patients with van Buchem disease. *J Med Genet* **39**: 91-97.
- Balemans, W., J. Van Den Ende, A. Freire Paes-Alves, F.G. Dikkers, P.J. Willems, F. Vanhoenacker, N. de Almeida-Melo, C.F. Alves, C.A. Stratakis, S.C. Hill, and W. Van Hul. 1999. Localization of the gene for sclerosteosis to the van Buchem disease-gene region on chromosome 17q12-q21. *Am J Hum Genet* **64**: 1661-1669.
- Beighton, P., J. Davidson, L. Durr, and H. Hamersma. 1977. Sclerosteosis - an autosomal recessive disorder. *Clin Genet* **11**: 1-7.
- Brunet, L.J., J.A. McMahon, A.P. McMahon, and R.M. Harland. 1998. Noggin, cartilage morphogenesis, and joint formation in the mammalian skeleton. *Science* **280**: 1455-1457.
- Brunkow, M.E., J.C. Gardner, J. Van Ness, B.W. Paeper, B.R. Kovacevich, S. Proll, J.E. Skonier, L. Zhao, P.J. Sabo, Y. Fu, R.S. Alisch, L. Gillett, T. Colbert, P. Tacconi, D. Galas, H. Hamersma, P. Beighton, and J. Mulligan. 2001. Bone dysplasia

- sclerosteosis results from loss of the SOST gene product, a novel cystine knot-containing protein. *Am J Hum Genet* **68**: 577-589.
- Chuzhanova, N., S.S. Abeysinghe, M. Krawczak, and D.N. Cooper. 2003. Translocation and gross deletion breakpoints in human inherited disease and cancer II: Potential involvement of repetitive sequence elements in secondary structure formation between DNA ends. *Hum Mutat* **22**: 245-251.
- Cimbora, D.M., D. Schubeler, A. Reik, J. Hamilton, C. Francastel, E.M. Epner, and M. Groudine. 2000. Long-distance control of origin choice and replication timing in the human beta-globin locus are independent of the locus control region. *Mol Cell Biol* **20**: 5581-5591.
- Curtin, P., M. Pirastu, Y.W. Kan, J.A. Gobert-Jones, A.D. Stephens, and H. Lehmann. 1985. A distant gene deletion affects beta-globin gene function in an atypical gamma delta beta-thalassemia. *J Clin Invest* **76**: 1554-1558.
- Curtin, P.T. and Y.W. Kan. 1988. The inactive beta globin gene on a gamma delta beta thalassemia chromosome has a normal structure and functions normally in vitro. *Blood* **71**: 766-770.
- Devlin, R.D., Z. Du, R.C. Pereira, R.B. Kimble, A.N. Economides, V. Jorgetti, and E. Canalis. 2003. Skeletal overexpression of noggin results in osteopenia and reduced bone formation. *Endocrinology* **144**: 1972-1978.
- Enattah, N.S., T. Sahi, E. Savilahti, J.D. Terwilliger, L. Peltonen, and I. Jarvela. 2002. Identification of a variant associated with adult-type hypolactasia. *Nat Genet* **30**: 233-237.

- Hamersma, H., J. Gardner, and P. Beighton. 2003. The natural history of sclerosteosis. *Clin Genet* **63**: 192-197.
- Ionasescu, V.V., C. Searby, R. Ionasescu, I.M. Neuhaus, and R. Werner. 1996. Mutations of the noncoding region of the connexin32 gene in X-linked dominant Charcot-Marie-Tooth neuropathy. *Neurology* **47**: 541-544.
- Khokha, M.K., D. Hsu, L.J. Brunet, M.S. Dionne, and R.M. Harland. 2003. Gremlin is the BMP antagonist required for maintenance of Shh and Fgf signals during limb patterning. *Nat Genet* **34**: 303-307.
- Kleinjan, D.A., A. Seawright, A. Schedl, R.A. Quinlan, S. Danes, and V. van Heyningen. 2001. Aniridia-associated translocations, DNase hypersensitivity, sequence comparison and transgenic analysis redefine the functional domain of PAX6. *Hum Mol Genet* **10**: 2049-2059.
- Kusu, N., J. Laurikkala, M. Imanishi, H. Usui, M. Konishi, A. Miyake, I. Thesleff, and N. Itoh. 2003. Sclerostin is a novel secreted osteoclast-derived bone morphogenetic protein (BMP) antagonist with unique ligand specificity. *J Biol Chem*.
- Lee, E.C., D. Yu, J. Martinez de Velasco, L. Tessarollo, D.A. Swing, D.L. Court, N.A. Jenkins, and N.G. Copeland. 2001. A highly efficient Escherichia coli-based chromosome engineering system adapted for recombinogenic targeting and subcloning of BAC DNA. *Genomics* **73**: 56-65.
- Lettice, L.A., S.J. Heaney, L.A. Purdie, L. Li, P. de Beer, B.A. Oostra, D. Goode, G. Elgar, R.E. Hill, and E. de Graaff. 2003. A long-range Shh enhancer regulates expression in the developing limb and fin and is associated with preaxial polydactyly. *Hum Mol Genet* **12**: 1725-1735.

- Mankoo, B.S., S. Skuntz, I. Harrigan, E. Grigorieva, A. Candia, C.V. Wright, H. Arnheiter, and V. Pachnis. 2003. The concerted action of Meox homeobox genes is required upstream of genetic pathways essential for the formation, patterning and differentiation of somites. *Development* **130**: 4655-4664.
- Mortlock, D.P., C. Guenther, and D.M. Kingsley. 2003. A general approach for identifying distant regulatory elements applied to the Gdf6 gene. *Genome Res* **13**: 2069-2081.
- Nobrega, M.A., I. Ovcharenko, V. Afzal, and E.M. Rubin. 2003. Scanning human gene deserts for long-range enhancers. *Science* **302**: 413.
- Ovcharenko, I., G.G. Loots, R.C. Hardison, W. Miller, and L. Stubbs. 2004. zPicture: dynamic alignment and visualization tool for analyzing conservation profiles. *Genome Res* **14**: 472-477.
- Petropoulos, H., P.J. Gianakopoulos, A.G. Ridgeway, and I.S. Skerjanc. 2004. Disruption of Meox or Gli activity ablates skeletal myogenesis in P19 cells. *J Biol Chem* **279**: 23874-23881.
- Sebat, J., B. Lakshmi, J. Troge, J. Alexander, J. Young, P. Lundin, S. Maner, H. Massa, M. Walker, M. Chi, N. Navin, R. Lucito, J. Healy, J. Hicks, K. Ye, A. Reiner, T.C. Gilliam, B. Trask, N. Patterson, A. Zetterberg, and M. Wigler. 2004. Large-scale copy number polymorphism in the human genome. *Science* **305**: 525-528.
- Stahling-Hampton, K., S. Proll, B.W. Paepfer, L. Zhao, P. Charmley, A. Brown, J.C. Gardner, D. Galas, R.C. Schatzman, P. Beighton, S. Papapoulos, H. Hamersma, and M.E. Brunkow. 2002. A 52-kb deletion in the SOST-MEOX1 intergenic

- region on 17q12-q21 is associated with van Buchem disease in the Dutch population. *Am J Med Genet* **110**: 144-152.
- Sutherland, M.K., J.C. Geoghegan, C. Yu, E. Turcott, J.E. Skonier, D.G. Winkler, and J.A. Latham. 2004. Sclerostin promotes the apoptosis of human osteoblastic cells: a novel regulation of bone formation. *Bone* **35**: 828-835.
- Tsui, F.W., H.W. Tsui, E.Y. Cheng, M. Stone, U. Payne, J.D. Reveille, M.J. Shulman, A.D. Paterson, and R.D. Inman. 2003. Novel genetic markers in the 5'-flanking region of ANKH are associated with ankylosing spondylitis. *Arthritis Rheum* **48**: 791-797.
- Uitterlinden, A.G., P.P. Arp, B.W. Paeper, P. Charmley, S. Proll, F. Rivadeneira, Y. Fang, J.B. van Meurs, T.B. Britschgi, J.A. Latham, R.C. Schatzman, H.A. Pols, and M.E. Brunkow. 2004. Polymorphisms in the sclerosteosis/van Buchem disease gene (SOST) region are associated with bone-mineral density in elderly whites. *Am J Hum Genet* **75**: 1032-1045.
- Van Bezooijen, R.L., B.A. Roelen, A. Visser, L. Van Der Wee-Pals, E. De Wilt, M. Karperien, H. Hamersma, S.E. Papapoulos, P. Ten Dijke, and C.W. Lowik. 2004. Sclerostin Is an Osteocyte-expressed Negative Regulator of Bone Formation, But Not a Classical BMP Antagonist. *J Exp Med* **199**: 805-814.
- Van Hul, W., W. Balemans, E. Van Hul, F.G. Dikkers, H. Obee, R.J. Stokroos, P. Hilderling, F. Vanhoenacker, G. Van Camp, and P.J. Willems. 1998. Van Buchem disease (hyperostosis corticalis generalisata) maps to chromosome 17q12-q21. *Am J Hum Genet* **62**: 391-399.

- Van Hul, W., F. Vanhoenacker, W. Balemans, K. Janssens, and A.M. De Schepper. 2001. Molecular and radiological diagnosis of sclerosing bone dysplasias. *Eur J Radiol* **40**: 198-207.
- Wang, H.L., T. Wu, W.T. Chang, A.H. Li, M.S. Chen, C.Y. Wu, and W. Fang. 2000. Point mutation associated with X-linked dominant Charcot-Marie-Tooth disease impairs the P2 promoter activity of human connexin-32 gene. *Brain Res Mol Brain Res* **78**: 146-153.
- Wergedal, J.E., K. Veskovic, M. Hellan, C. Nyght, W. Balemans, C. Libanati, F.M. Vanhoenacker, J. Tan, D.J. Baylink, and W. Van Hul. 2003. Patients with Van Buchem disease, an osteosclerotic genetic disease, have elevated bone formation markers, higher bone density, and greater derived polar moment of inertia than normal. *J Clin Endocrinol Metab* **88**: 5778-5783.
- Winkler, D.G., M.K. Sutherland, J.C. Geoghegan, C. Yu, T. Hayes, J.E. Skonier, D. Shpektor, M. Jonas, B.R. Kovacevich, K. Staehling-Hampton, M. Appleby, M.E. Brunkow, and J.A. Latham. 2003. Osteocyte control of bone formation via sclerostin, a novel BMP antagonist. *Embo J* **22**: 6267-6276.
- Winkler, D.G., C. Yu, J.C. Geoghegan, E.W. Ojala, J.E. Skonier, D. Shpektor, M.K. Sutherland, and J.A. Latham. 2004. Noggin and sclerostin bone morphogenetic protein antagonists form a mutually inhibitory complex. *J Biol Chem* **279**: 36293-36298.

FIGURE LEGENDS

Figure 1. Generation and Characterization of Van Buchem transgenic mouse models.

(A) A 158kb human BAC (hSOST^{wt}) spanning *sost* and *meox1* was engineered using *in vitro* BAC recombination in *E.coli* (Lee et al. 2001) by deleting the 52kb noncoding region missing in VB patients (hSOST^{vbΔ}). Human *sost* expression was analyzed by rtPCR in adult tissues (B) and quantitative rtPCR in E10.5 embryos (C) from two independent lines of each hSOST^{wt} and hSOST^{vbΔ} transgene.

Figure 2. *Sost* transgenic expression negatively impacts bone parameters. (A) Body weight measurements of 5-month-old male mice (non-tg = 13, hSOST^{wt} = 15, hSOST^{vbΔ} = 14; animals were pooled from two lines of hSOST^{wt} and two lines of hSOST^{vbΔ}; Supplementary Materials). (B) Bone mineral density in the tibia, femur and lumbar spine as evaluated by DEXA. (C) Bone volume, trabecular number, thickness and separation as evaluated in the cancellous bone compartment of the proximal tibia metaphysis by μ CT. (Mean +/- SEM; * p<.05 versus non-tg).

Figure 3. Human *sost* dose effect on bone metabolism in the proximal tibia metaphysis of 5-month-old male mice (non-tg = 5, hSOST^{wt/+} = 7, hSOST^{wt/wt} = 4). (A) Bone volume and (B) bone formation rates as determined by μ CT scans and histomorphometric analysis respectively. (Mean +/- SEM; * p<.05 versus non-tg; x p<.05 versus hSOST^{wt/+}). (C) Cancellous bone compartment of non-transgenic and hSOST^{wt/wt} mice. (D) Fluorochrome marker uptake at site of active mineralization of bone matrix laid down by

osteoblasts in wildtype and transgenic mice at the interface between endocortex and cancellous bone.

Figure 4. Embryonic *sost* expression and limb deformity in hSOST^{wt} and hSOST^{vba} transgenic mice. High levels of embryonic *sost* expression was predominantly detected in the developing limb bud of E10.5 defective mice, as visualized by whole mount *in situ* hybridization using a *sost* probe that detects human and mouse transcripts (A). μ CT scans of defective hSOST^{wt} and hSOST^{vba} adult limbs overexpressing human *sost* (B).

Figure 5. Enhancer activity of evolutionarily conserved noncoding sequences from the Van Buchem deletion region. (A) Human/Mouse genomic alignment generated using zPicture alignment engine (<http://zpicture.dcode.org/>). Exons are in blue, untranslated regions in yellow, repetitive elements in green and noncoding sequences in red (intragenic) or pink (intronic). Seven highly conserved elements (≥ 200 bp; $\geq 80\%$ ID; ECR2-8) within VBA and the promoter region were tested in rat-osteosarcoma (UMR-106) and kidney cells (293) for the ability to enhance luciferase expression from the SV40-promoter (B) or human *sost* promoter (C). ECR5 activates the human *sost* promoter in rat osteosarcoma cells (C), and drives the *hsp68* promoter in the skeleton of E14.5 mouse embryos (D).

Figure 1

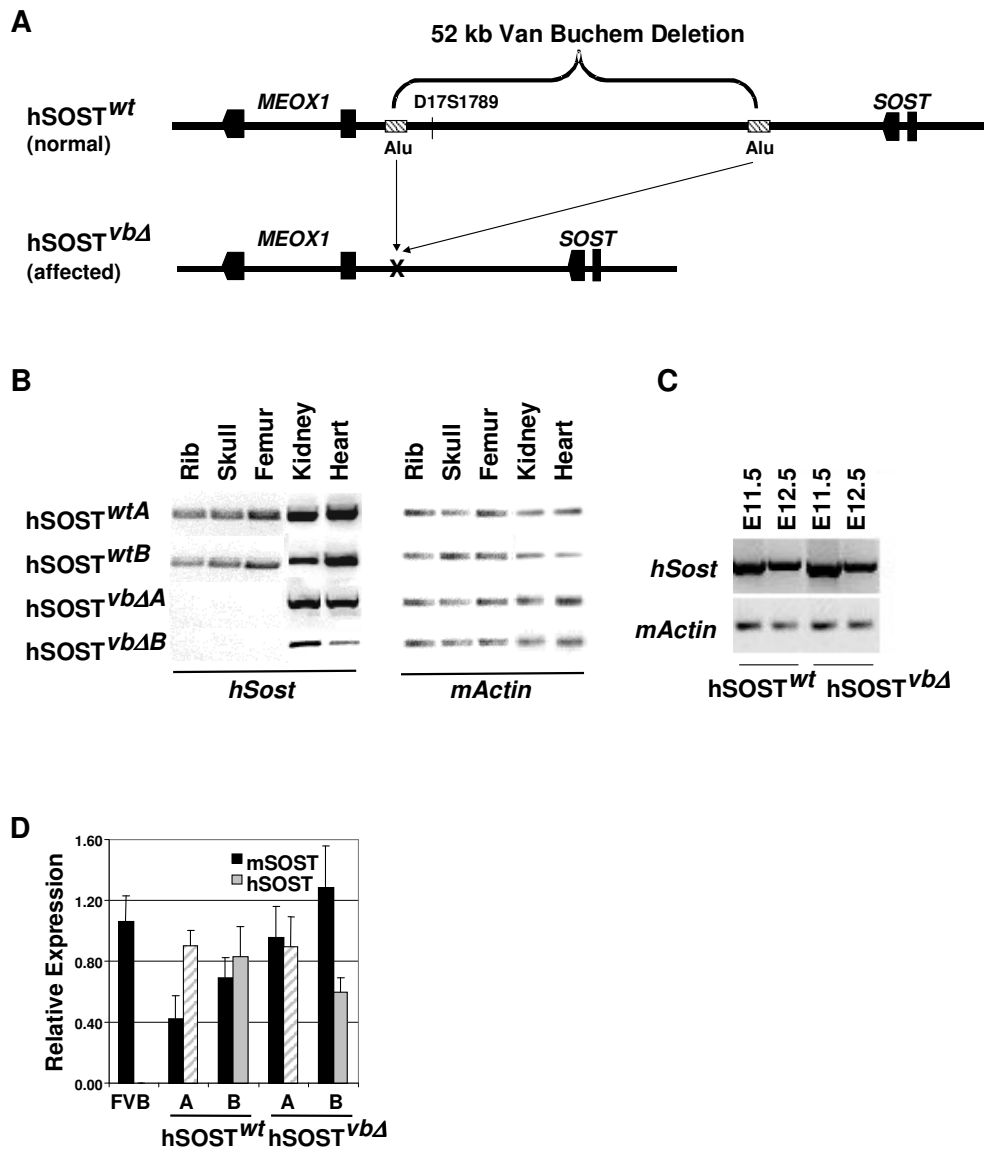


Figure 2

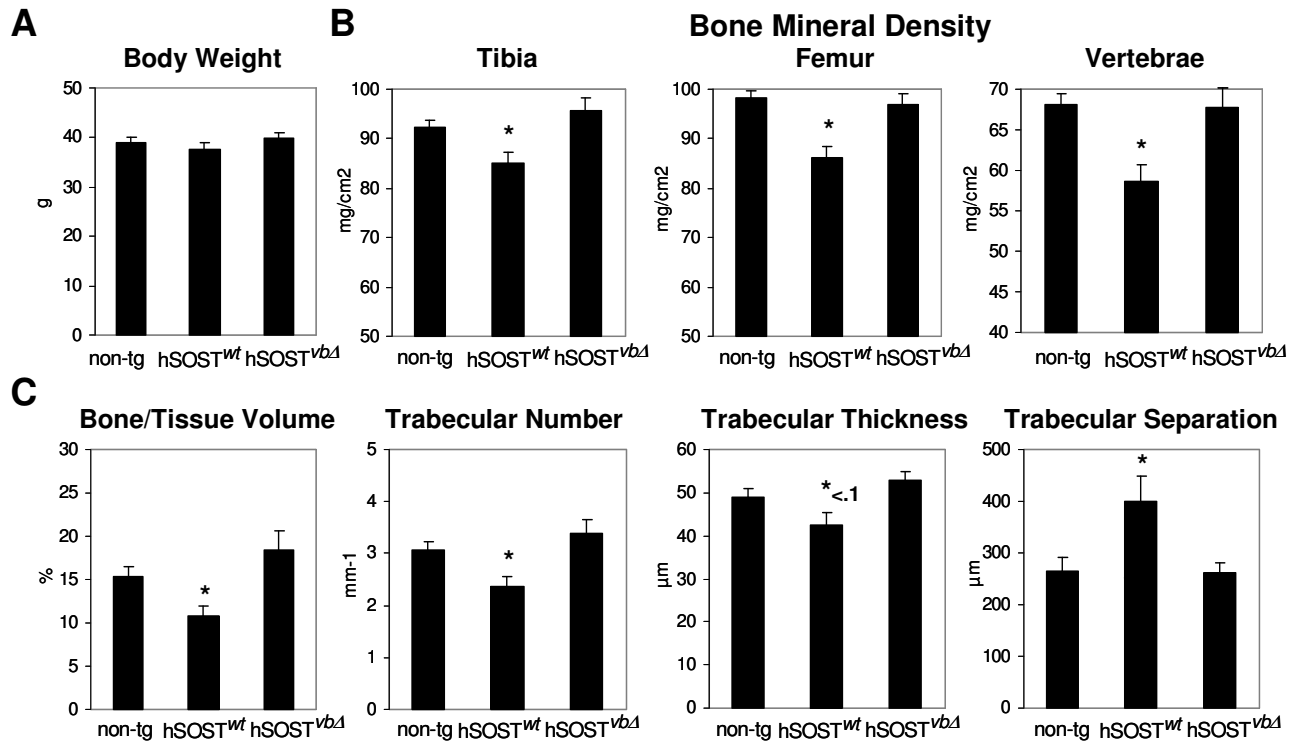


Figure 3

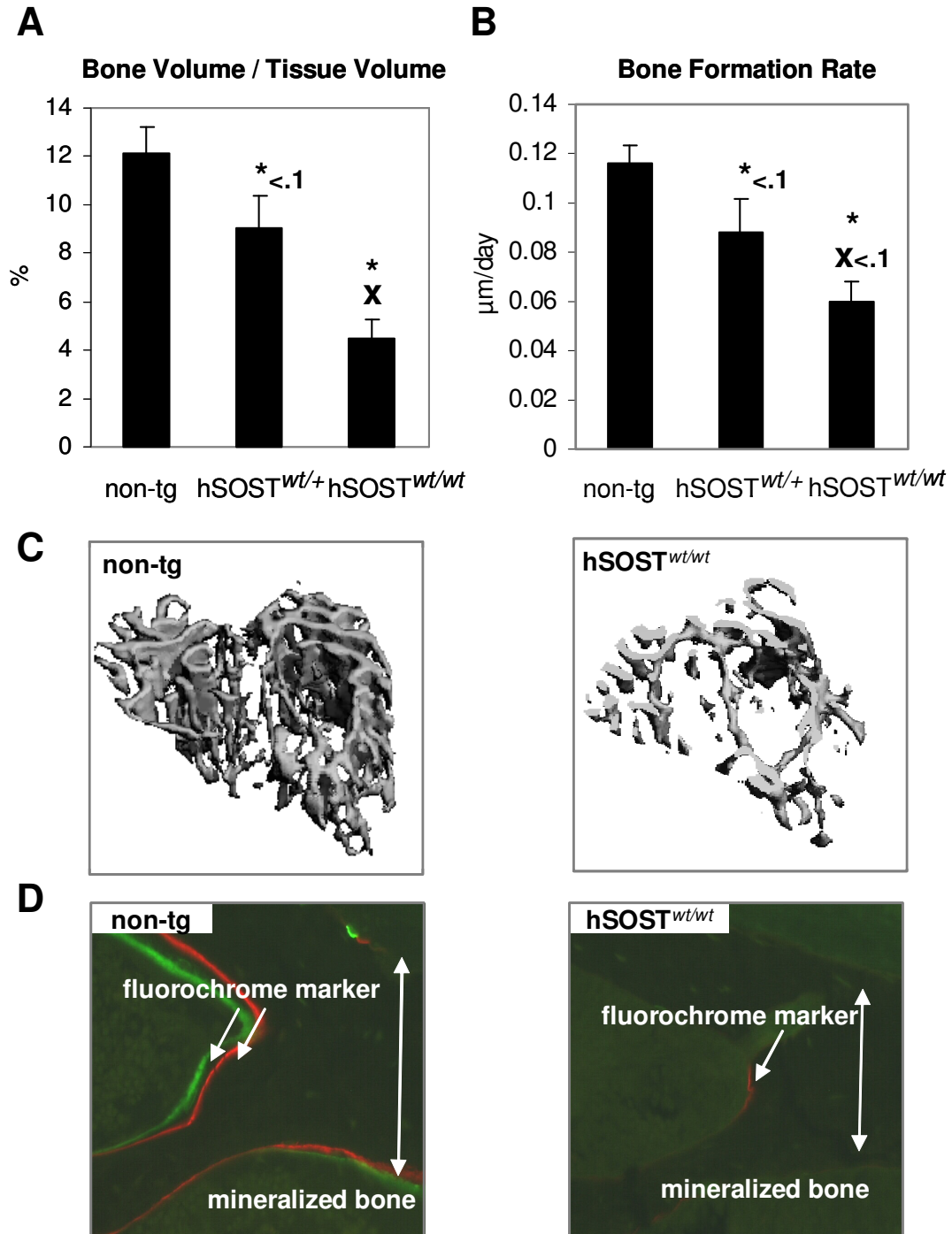
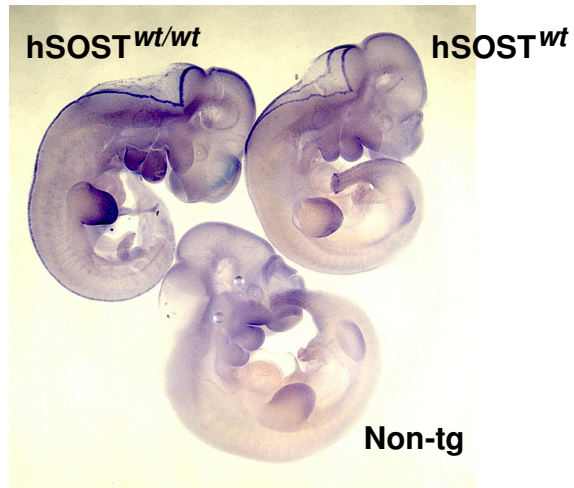


Figure 4

A



B

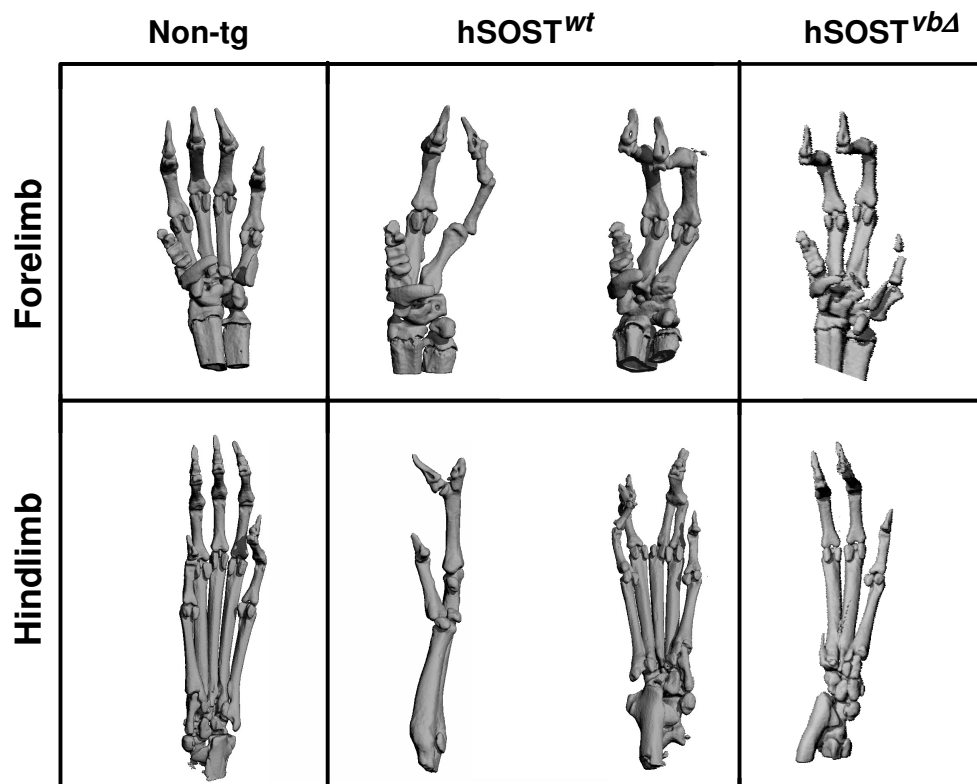


Figure 5

